Journal of
Chemical Engineering & Process Technology

Esfandyari et al., J Chem Eng Process Technol 2012, 3:1
DOI: 4172/2157-7048.1000124

Research Article Open Access

Modeling of Cu Doped Cobalt Oxide Nanocrystal Gas Sensor for Methane Detection: ANFIS Approach

A. Ahmadpour[1], Z. Sheikhi Mehrabadi[1], J.R. Esfandyari[2]* and M. Koolivand-Salooki[3]

[1]*Department of Chemical Engineering, Faculty of Engineering, Ferdowsi University of Mashhad, Khorasan, Iran*
[2]*The Technical teacher of saveh education office, saveh, Iran*
[3]*Department of Chemical Engineering, omideh beranch, Islamic Azad University, omideh, Iran*

Abstract

In this paper, Nano-sized copper-cobalt compound oxide powders have been prepared by sol-gel technique with different mole ratios of Cu/Co (from 0.00 to 0.15); Detection of the methane gas, the most chemically stable hydrocarbon, is done. The structural properties and morphology of powders were studied by X-ray diffraction (XRD), Fourier transform infrared spectroscopy (FTIR) and Transmission electron microscopy (TEM). XRD analysis confirms that Co_3O_4 and $(CuO_{0.3}CO_{0.7})$ Co_2O_4 phases have been formed and mean grain size were decreased with increasing dopant (from 28 to 24nm). According to TEM images it was found that the particles have cubic morphologies with nearly uniform distribution. Then an adaptive neuro-fuzzy inference system (ANFIS) models have been utilized for prediction of sensitivity values of the corresponded sensor. The results of ANFIS model show that the independent predicted Sensitivity values (S) compared to the measured target values have a good agreement. And also, high coefficient were found ($R^2 > 0.98$) for the response.

Keywords: Nano particles; Cu/Co; ANFIS; XRD; TEM; FTIR

Introduction

Methane (CH_4) is a major component of the widely used natural fuel gases in the industry and the private household. Explosion will occur when its concentration in air reaches to 5-16% (v/v); therefore the monitoring of CH_4 in the industry is very important for safety reasons. In addition, it is also one of the greenhouse gases which are produced continuously by the anaerobic oxidation of organic materials, so it needs to be monitored. However, CH_4 is relatively difficult to detect at ambient conditions because its chemical reactivity is relatively low. The commonly used techniques for CH_4 detection include gas chromatography (GC) [1-9], semiconductor devices [10-21], optical fiber sensors [22], electrochemical methods [23-24], and biochemical methods [25, 26].

Many Nano-sized pure and doped semiconducting oxides have been used for gas sensors [27-30]. Use of Nano-materials is interested because of much greater surface area to the bulk ratio rather than course materials. In addition, when the grain size reduce to nanometer, especially when the dimensions become less than two times of the space-charge depth, a large fraction of atoms which will present in the surface and the surface properties become dominant. So, materials conduction type turns to surface conduction type [31-33]. The sensing mechanism depends on the changes in surface conductivity which is resulted from chemical reaction between target gases and the absorbed oxygen on the surface of the Nano-sized metal oxide. Consequently, it is important to enhance the rate of chemisorptions and surface reaction. Co_3O_4 is most active catalyst for oxidation of the methane [34]. So, it is a good candidate for the methane gas sensor. Addition of second component as doping is becoming one of the most interesting methods for optimization of the gas sensing properties in this type of sensors. These additives can act as catalysts in surface sites for adsorption of oxygen and detected gas or as promoters of the gas sensing characteristics [35]. The copper oxide has good catalytic activity for oxidation of the methane [34], so it was used as dopant for the methane gas sensor. For this reason, in this research, Nano-sized Cu- doped Cobalt oxides with different concentrations of the dopant have been prepared by the sol-gel method for the methane sensor application.

Material and Methods

The present paper covers an ANFIS modeling and experimental study of the gas sensing of the copper-cobalt compound oxide Nano particles. Experimental measurements have been made and Nano-sized powders have been prepared by the sol-gel technique with different mole ratios of the Cu/Co (from 0.05 to 0.15) for detection of the methane gas. The structural properties and morphology of the powders were studied by the X-ray diffraction (XRD), Fourier transform infrared spectroscopy (FTIR) and Transmission electron microscopy (TEM).

Adaptive network based fuzzy inference system

The ANFIS is a fuzzy Sugeno model placed in the framework of adaptive systems to facilitate learning and adaptation [36]. Sugeno type fuzzy inference systems (FIS) use a combination of least-squares and back propagation gradient descent methods, along with a hybrid learning algorithm to identify the membership function parameters and fuzzy IF–THEN rules based on a single output or singleton [37].

ANFIS represents a useful neural network approach for the solution of function approximation problems [38].

ANFIS structure For simplicity, it is assumed that the fuzzy inference system under consideration has two inputs and one output. The rule base contains two fuzzy if-then rules of Takagi and Sugeno's type [39] as follows:

***Corresponding author:** J.R. Esfandyari, The technical teacher of saveh education office, saveh, Iran, Tel: +989361187489; Fax: +98 5118816840; E-mail: m_s_13611364@yahoo.com

Received October 31, 2011; **Accepted** February 22, 2012; **Published** February 27, 2012

Citation: Ahmadpour A, Mehrabadi ZS, Esfandyari JR, Koolivand-Salooki M (2012) Modeling of Cu Doped Cobalt Oxide Nanocrystal Gas Sensor for Methane Detection: ANFIS Approach. J Chem Eng Process Technol 3:124. doi:10.4172/2157-7048.1000124

Citation: Ahmadpour A, Mehrabadi ZS, Esfandyari JR, Koolivand-Salooki M (2012) Modeling of Cu Doped Cobalt Oxide Nanocrystal Gas Sensor for Methane Detection: ANFIS Approach. J Chem Eng Process Technol 3:124. doi:10.4172/2157-7048.1000124

If x is A and y is B then z is f(x, y)

Where A and B are the fuzzy sets in the antecedents and z = f (x, y) is a crisp function in the consequent. f(x, y) is usually a polynomial for the input variables x and y.

Consider z= f (x, y) is a first-order Sugeno fuzzy inference system, which contains two rules.

Rule 1: If x is A_1 and y is B_1, Then: $f_1 = a_1 x + b_1 y + c_1$

Rule 2: If x is A_2 and y is B_2, Then: $f_2 = a_2 x + b_2 y + c_2$

ANFIS structure contains five layers excluding input layer.

Layer 0 is the input layer. It has n nodes where n is the number of inputs to the system.

Layer 1 is the fuzzification layer in which each node represents a generalized bell curve membership function value of a linguistic term as follows:

$$\mu_A(x) = \frac{1}{1 + \left| \frac{x - c_i}{a_i} \right|^{2b_i}} \quad (1)$$

Each node in Layer 2 provides the strength of the rule by means of multiplication operator. It performs AND operation.

Layer 3 is the normalization layer which normalizes the strength of all the rules according to the following equation:

$$O_{3,i} = \overline{w_i} = \frac{w_i}{w_1 + w_2} \quad i=1, 2 \quad (2)$$

Layer 4 is a layer of adaptive nodes. Every node in this layer computes a linear function where the function coefficients are adapted by using the error function of the multilayer feed-forward neural network.

Layer 5 is the output layer whose function is the summation of the net outputs of the nodes in Layer 4. The output f is computed as follows in Figure 1:

The first layer, every node i in this layer is an adaptive node with node function in Equation 1:

$$\mu_{\mathrm{Ai}}(x) = e^{-((x - x^*)/\sigma^2)} \quad (3)$$

Where {x*} are σ premise parameters updated through hybrid learning algorithm and x is input variable. At least in the basic ANFIS method these parameters are not adjustable.

The second layer calculates the firing strength for each rule quantifying the extent which any input data belongs to that rule. The output of the layer is the algebraic product of the input signals as can be given as: [40-42]

$$O_{2,i} = \omega_i = \mu_{\mathrm{Ai}}(x_1) \times \ldots . \times \mu_{Ci}(x_n) \quad (4)$$

Figure 2 shows the ANFIS structure of T, Q and Ratio Cu/Co values as the three input parameters and two linguistic values (healthy or bruised) as the output parameters. After training the ANFIS model, predicted performance was tested.

Experimental

Nano-particles of copper-cobalt compound oxides were synthesized by sol-gel method. Systematically a proper amount of $CoCl_2.6H_2O$ and $CuCl_2.2H_2O$ dissolved in deionized water and ethanol. The initial solutions have been prepared with mole ratios of Cu/Co = 0.0, 0.05, 0.08, 0.10, 0.125 and 0.15. Then, citric acid (as complexing agent) was added in a mole ratio of $C_6H_8O_7/CoCl_2.6H_2O = 5$, and primary sol was prepared by adding ethylene glycol (as polymerizing agent) in the mole ratio six time over cobalt cation and was stirred for 20 minutes. The clear mixed solution was refluxed at 120°C in oil bath for 6 hours. The final sol ensuing from reflux was kept at 80°C for 17 hours in oil bath to evaporate volatile compounds and a wet gel was formed. For removing the other residual volatile component the gel was heated again directly on hotplate at 180°C for 3 hours and then 220°C for 30 minutes. Finally the dry gel was annealed in 450°C for 1 hour to eliminate organic component and the copper-cobalt oxides Nano-powder was obtained. For gas sensing measurements, usually nanopowders screen-printed on the electrodes. So, using a component as binder, in many cases ethylene glycol, is necessary. Choi and Min [34] reported that sensitivity of a Co_3O_4 sensor decreases with increasing of the ethylene glycol. Accordingly, sensors were fabricated by pressing followed by hot treatment. The same amount of each powders were pressed into pellets at a pressure of 7 ton and then heated in furnace for 2 hours at 800°C with heating rate of 2°C/min. Silver paste was used as electrodes on the two sides of one surface of pellets for recording of the resistant change.

Phase formation and crystallinity were studied by X-ray diffraction using a D8 Advanced Bruker with Cu kα radiation (λ=0.15405 nm) in a 2θ range from 15° to 85° with a step size of 0.05°. The atomic link

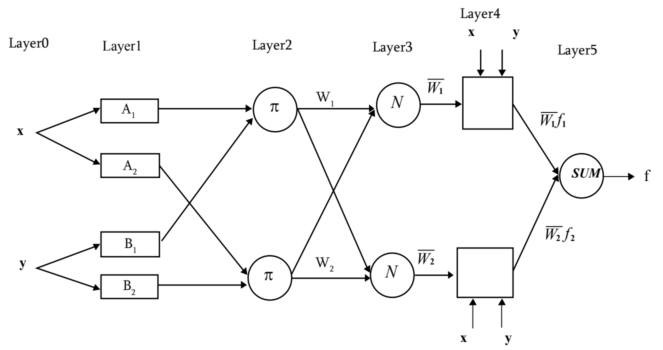

Figure 1: Basic ANFIS Structure.

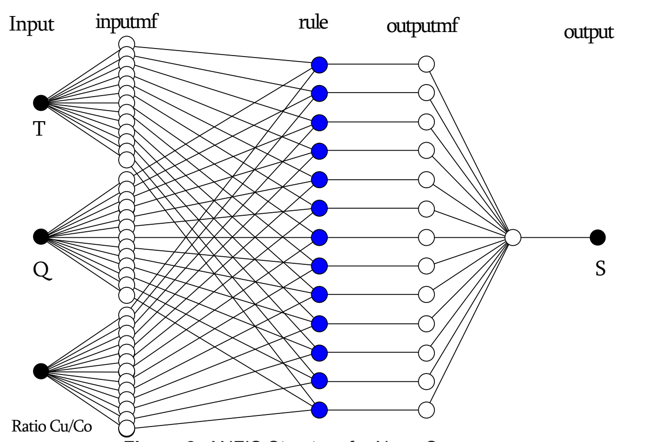

Figure 2: ANFIS Structure for Nano Sensor.

investigation was performed using Fourier transform infrared (FTIR) spectroscopy on a Bomem MB-154 spectrometer. Transmission electron microscopy (TEM) was carried out on a LEO 912 AB transmission electron microscope for determination of the particle shape and size. The prepared sensors were located in the testing chamber for gas sensing characterization. All sensitivity measurements were done in constant temperature in the range of 200-300°C and fixed quantity of sample gas of methane (3000 to 6000ppm). Electrical resistance of the sensor was monitored by a digital multimeter.

The sensitivity was defined as

$(R_{gas}-R_{air})/R_{air}\times 100(\%)$

Where R_{air} and R_{gas} are the electrical resistance in clean air and in presence of the gas at the same temperature, respectively.

Result and Discussion

Experimental results

The XRD patterns of copper-cobalt oxides nanopowders with different mole ratio of copper have been shown in Figure 3. It reveals polycrystalline structure consisting of cubic Co_3O_4 (a=8.08400Å) in all samples and $(CuO_{0.3}CoO_{0.7})\ Co_2O_4$ in which contain Cu.

Major XRD peaks are corresponded to (3 1 1) plane at 36.9° and it intensity does not change evidently by adding copper impurity in samples but it has become slight wider. Beside the strongest peak, also other peaks corresponded to (2 2 0) and (4 4 0) planes have got wider. It's clearly identified that copper impurity decreases the crystallinity and enhances the amorphous state that lead to the decreasing of the crystalline size. No other phase has been created in samples with different Cu/Co mole ratios and it demonstrates that formed phase are stable and its formation is independent of copper quantity.

Mean particle's size in major peaks is calculated using Scherrer's equation.

$$D = \frac{k\lambda}{\beta\cos\theta} \tag{5}$$

Where k is constant, depend on crystal morphology in the range of 0.89-1.39 and it is 0.9 in this calculation. λ is the x-ray wavelength, β is the line broadening at half the maximum intensity (FWHM) in radians and θ is the Brrag angle of XRD peak. The particle size values are given in Table 1. It was varied between 24 and 28 and decrease as Cu/Co mole ratio increase to 0.15.

Figure 4 shows FTIR spectra of copper-cobalt oxide Nano-particles with different mole ratios of Cu/Co = 0.0, 0.05, 0.10, 0.15 (S_1, S_2, S_4 and S_6 respectively).

The bands at 576 and 668 cm^{-1} are attributed to vibration of Co-O in the Co_3O_4. Any peak related to Cu-O could not be identified; it is probably Co-O peaks overlap Cu-O peak, and they have seen in very close wavelength. There is no peak that could be assigned to C-H which suggests that carbonate component removed completely from samples.

TEM images of cobalt oxide nanoparticles (S_1) and copper-cobalt oxide nanoparticles with Cu/Co = 0.15 (S_6) prepared by sol- gel method with different magnification are given in Figure 5.

It's found that particles have cubic morphologies with uniform distribution. The average particle size was 30 nm in S_1 and 15nm in S_6 which decreases by increasing of the dopant. It has a good agreement with result of Scherre's formula.

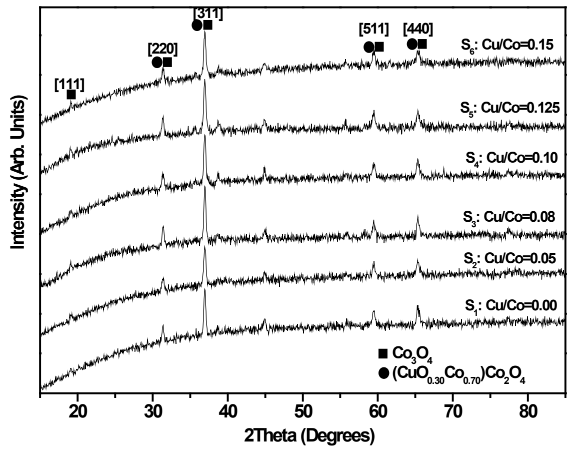

Figure 3: XRD patterns of Cu-Co oxides nano-particles with different Cu/Co mole ratio.

Sample	Mole ratio Cu/Co	2θ°	β	D(nm)
S_1	0.00	36.95	0.295	28
S_2	0.05	36.95	0.337	27
S_3	0.08	37.025	0.304	27
S_4	0.10	37.075	0.314	26
S_5	0.125	37.125	0.328	25
S_6	0.15	37.00	0.335	24

Table 1: The X-Ray Parameters and Particles Mean Size of Cu-Co Oxides Nano-Particles with Different Mole Ratios of Cu/Co Prepared By Sol-Gel Method.

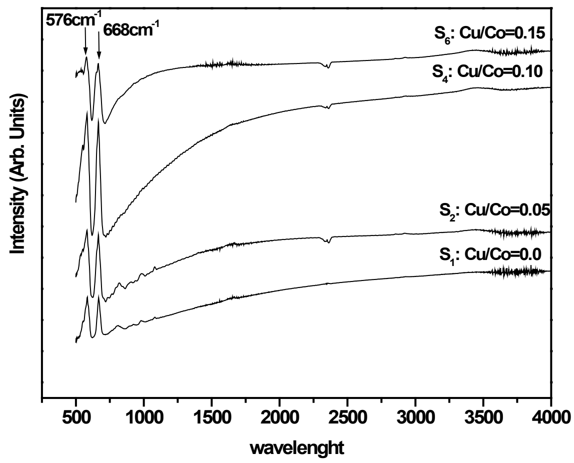

Figure 4: FT-IR Intensity Results for Cu-Co Oxides Nano-Crystals with Different Cu/Co Mole Ratios.

ANFIS comparative analyses and discussion

Two models of Sugeno, with an automatic extraction of data from FIS [GENFIS2] were used. The MATLAB software was adopted for comparison purposes. Moreover, the coverage threshold was fixes to 0.01. Table 2 shows experimental data and predicted data by ANFIS.

3D surface plots for the sensitivity values of nano sensor showing

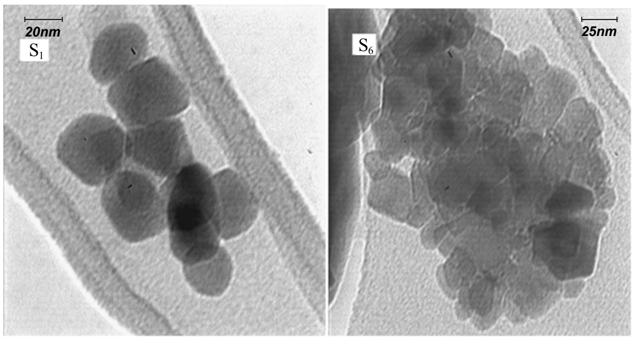

(a) (b)

Figure 5: TEM images for Cu-Co oxides nano-crystals with different Cu/Co mole ratios prepared by sol-gel method; (a) Cu/Co mole ratio=0.0, (b) Cu/Co mole ratio=0.15.

No.	T	Q (ppm)	Cu/Co	Experimental S	predicted S
Train data					
1	200	3000	0	0.1	0.103321
2	300	4500	0	7.2	7.154434
3	300	3000	0.05	2.5	2.418407
4	250	3000	0.05	1.3	1.340887
5	200	6000	0.08	4.1	4.164952
6	250	6000	0.08	5.3	5.377992
7	300	6000	0.1	23	22.28085
8	250	4500	0.1	5.9	5.87822
9	200	4500	0.125	2.9	2.870968
10	200	3000	0.15	2.2	2.177522
11	300	4500	0.15	23.9	21.86092
12	300	3000	0	0.4	0.392231
13	250	3000	0	0.2	0.20146
14	200	6000	0.05	3.8	3.538453
15	250	6000	0.05	4.4	4.177549
16	300	6000	0.08	19.7	20.136
17	250	4500	0.08	4.5	4.571422
18	200	4500	0.1	4.3	4.280648
19	200	3000	0.125	1.9	1.937442
20	300	4500	0.125	15.3	19.44232
21	300	3000	0.15	11.6	11.21666
22	250	3000	0.15	4.2	4.852579
23	200	6000	0	0.6	0.617481
24	250	6000	0	1.1	1.16363
25	300	6000	0.05	16.1	16.09997
26	250	4500	0.05	3.8	3.79999
27	200	4500	0.08	3.8	3.869347
28	200	3000	0.1	1.7	1.693322
29	300	4500	0.1	19.2	18.98301
30	300	3000	0.125	10.4	9.472365
31	250	3000	0.125	4.9	4.87564
32	200	6000	0.15	4.1	4.198856
33	250	6000	0.15	10.6	10.68818
34	200	4500	0	0.4	0.4
35	200	3000	0.05	1.1	1.08839
36	300	4500	0.05	12.5	12.65927
37	300	3000	0.08	5	4.86945
38	250	3000	0.08	2	2.02037
39	200	6000	0.1	5	4.953835
40	250	6000	0.1	7.4	7.39907
41	300	6000	0.125	25.3	25.58313
42	250	4500	0.125	7.6	7.646367
43	200	4500	0.15	4	3.961449
Test data					
44	300	6000	0	8.9	8.755444
45	250	4500	0	0.9	1.013
46	200	4500	0.05	3.2	3.11
47	200	3000	0.08	1.5	1.534764
48	300	4500	0.08	14.8	15.03857
49	300	3000	0.1	6.2	6.681882
50	250	3000	0.1	2.5	2.488226
51	200	6000	0.125	3.7	3.81
52	250	6000	0.125	8.9	8.854872
53	300	6000	0.15	31.1	29.97888
54	250	4500	0.15	8.9	9.01223

Table 2: Comparison of Experimental Data with Predicted Values for S.

the relationship between Temperature, Q, ratio Cu/Co and S are given in Figure 6:

A complete graphical comparison of experimental data used for testing or validating the predictions of ANFIS models are shown in Figures 7&8 for the train and the test data respectively. The coefficient of determination values (R^2), which quantifies the degree of agreement between experimental observations and numerically calculated values were found greater than 0.96 for all output variables are shown in Figure 9&10. R^2 was defined as below:

$$R^2 = \frac{\sum_{i=1}^{N}(x_i - \bar{x})(y_i - \bar{y})}{\sqrt{\sum_{i=1}^{N}(x_i - \bar{x})^2}\sqrt{\sum_{i=1}^{N}(y_i - \bar{y})^2}} \tag{6}$$

Table 3 reveals average relative error (ARE), absolute average relative error (AARE) and root mean square error (RMSE) for Nano Cu/Co respectively. ARE, AARE and RMSE are defined as below:

$$ARE = \frac{1}{N}\sum_{i=1}^{N}\left(\frac{X_{experimental(i)} - X_{caculated(i)}}{X_{experimental(i)}}\right) \tag{7}$$

$$AARE = \frac{1}{N}\sum_{i=1}^{N}\left(\left|\frac{X_{experimental(i)} - X_{caculated(i)}}{X_{experimental(i)}}\right|\right) \quad (8)$$

$$\text{RMSE} = \sqrt{\frac{\sum_{i=1}^{n}(X_{experimental(i)} - X_{caculated(i)})^2}{n}} \quad (9)$$

Conclusion

Copper-cobalt oxide Nano-sized powders with different mole ratio of Cu/Co from 0.0 to 0.15 were prepared by sol-gel technique for gas sensor application. Cubic Co_3O_4 and $(CuO_{0.3}CoO_{0.70})$ Co_2O_4 phases were firmly formed. The mean grain size varied from 28 to 24 by changing Cu/Co mole ratios from 0.0 to 0.15. The gas sensing performances of sensors were investigated in presence of methane gas. The results have shown that optimal operating temperature is 300°C in all sensors. Doping of metal oxide to Co_3O_4 altered the sensing behavior by influence defect chemistry and decrease particle size. The performance of the ANFIS Prediction and experimental results was measured using the average relative error (ARE), absolute average relative error (AARE), root mean square error (RMSE) and the Coefficients (R^2) values. The developed ANFIS model showed a good regression analysis with the R^2 greater than 0.98. As the regression coefficients indicate the ANFIS approach could be considered as an alternative and practical technique to evaluate the sensitivity (S) based on the Q, temperature and ratio of Cu/Co with a high degree of accuracy.

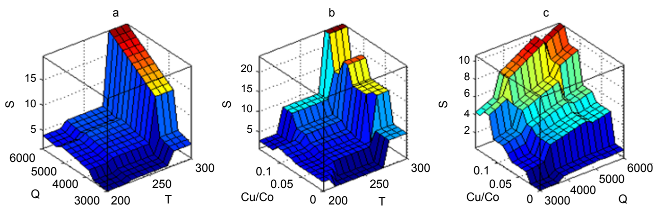

Figure 6: 3D surface plots for the sensitivity values of nano sensor.

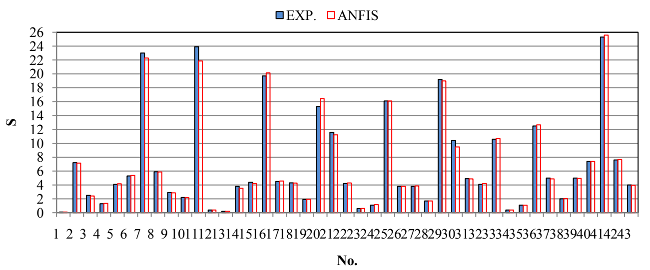

Figure 7: Comparison between the ANFIS modeling of this work and experimental data for train data.

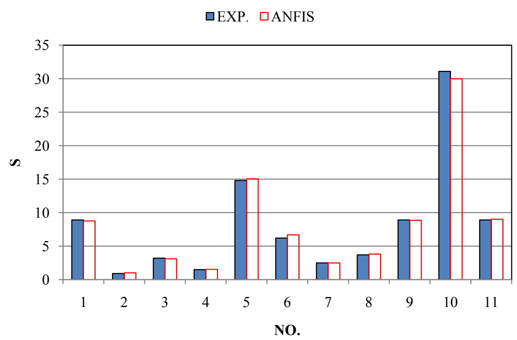

Figure 8: Comparison between the ANFIS modeling of this work and experimental data for test data.

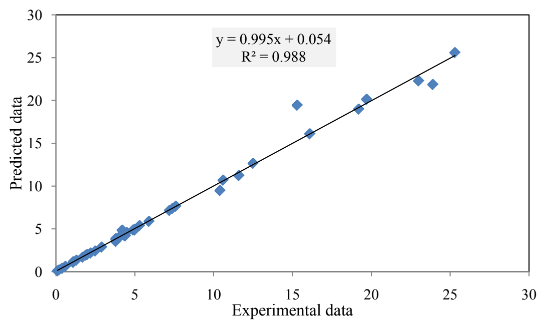

Figure 9: Comparison between of experimental data with predicted values for train data.

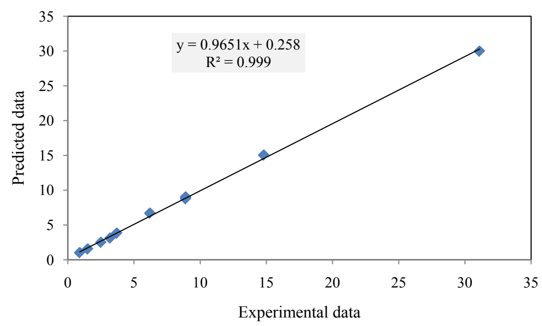

Figure 10: Comparison between of experimental data with predicted values for test data.

	Method	%ARE	%AARE	RMSE
Train	ANFIS	-0.56	2.98	0.74
Test	ANFIS	-1.77	3.41	0.38

Table 3: ARE, AARE and RMSE for nano sensor which modeled by ANFIS.

References

1. Hugon O, Sauvan M, Benech P, Pijolat C, Lefebvre F (2000) Gas separation with a zeolite filter, application to the selectivity enhancement of chemical sensors. Sens Actuators B 67: 235-243.
2. Ohta K, Terai H, Kimura I, Tanaka K (1999) Simultaneous Determination of Hydrogen, Methane, and Carbon Monoxide in Water by Gas Chromatography with a Semiconductor Detector. Anal Chem 71: 2697-2699.
3. Janicki W, Chrzanowski W, Zwan P, Namieśnik J (2003) Automated analyser for monitoring the contents of hydrocarbons in gas emitted from exploratory bore-holes in the gas and oil industry. J Autom Methods Manag Chem 25: 141-147.
4. Hansen TL, Schmidt JE, Angelidaki I, Marca E, Jansen JC et al. (2004) Method for determination of methane potentials of solid organic waste. Waste Manag 24: 393-400.
5. Forsyth DS (2004) Pulsed discharge detector: theory and applications. J Chromatogr A 24: 63-68.

6. Maris C, Chung MY, Lueb R, Krischke U, Meller R, et al. (2003) Development of instrumentation for simultaneous analysis of total non-methane organic carbon and volatile organic compounds in ambient air. Atmos Environ 37: 149-158.

7. Raksit A, Johri S (2003) Determination of dissolved volatile hydrocarbons in environmental aqueous samples by headspace-gas chromatography with flame ionization detection. Am Lab 35: 10-13.

8. Kamiński M, Kartanowicz R, Jastrzebski D, Kamiński MM (2003) Determination of carbon monoxide, methane and carbon dioxide in refinery hydrogen gases and air by gas chromatography. J Chromatogr A 989: 277-283.

9. Worthy DEJ, Levin I, Trivett NBA, Kuhlmann AJ, Hopper JF, et al. (1998) Seven years of continuous methane observations at a remote boreal site in Ontario, Canada. J Geophys Res 103: 15995-16007.

10. Seiyama T, Kato A, Fujiishi K, Nagatani M (1962) A new detector for gaseous components using semiconductive thin films. Anal Chem 34: 1502-1503.

11. Fleischer M, Kornely S, Weh T, Frank J, Meixner H (2000) Selective gas detection with high-temperature operated metal oxides using catalytic filters. Sens Actuators B 69: 205-210.

12. Faglia G, Comini E, Sberveglieri G, Rella R, Siciliano P, et al. (1998) Square and collinear four probe array and Hall measurements onmetal oxide thin film gas sensors. Sens Actuators B 53: 69-75.

13. Benounis M, Jaffrezic-Renault N, Dutasta JP, Cherif K, Abdelghani A (2005) Study of a new evanescent wave optical fibre sensor for methane detection based on cryptophane molecules. Sens Actuators B 107: 32-39.

14. Tournier G, Pijolat C (1999) Influence of oxygen concentration in the carrier gas on the response of tin dioxide sensor under hydrogen and methane. Sens Actuators B 61: 43-50.

15. Llobet E, Orts J, Vilanova X, Brezmes J, Correig X (1999) Selective methane detection under varying moisture conditions using static and dynamic sensor signals. Sens Actuators B 60: 106-117.

16. Pijolat C, Pupier C, Sauvan M, Tournier G, Lalauze R (1999) Gas detection for automotive pollution control. Sens Actuators B 59: 195-202.

17. Quaranta F, Rella R, Siciliano P, Capone S, Epifani M, et al. (1999) A novel gas sensor based on SnO_2 thin film for the detection of methane at low temperature. Sens Actuators B 58: 350-355.

18. Licznerski BW, Nitsch K, Teterycz H, Szecˇıowka PM, Wisniewski K (1999) Humidity insensitive thick film methane sensor based on SnO_2/Pt. Sens Actuators B 57: 192-196.

19. Schmid W, Barsan N, Weimar U (2003) Sensing of hydrocarbons with tin oxide sensors: possible reaction path as revealed by consumption measurements. Sens Actuators B 89: 232-236.

20. Gajdosik L (2002) The derivation of the electrical conductance/concentration dependency for SnO_2 gas sensor for ethanol. Sens Actuators B 81: 347-350.

21. Saha M, Banerjee A, Halder AK, Mondal J, Sen A, et al. (2001) Effect of alumina addition on methane sensitivity of tin dioxide thick films. Sens Actuators B 79: 192-195.

22. Llobet E, Rubio J, Vilanova X, Brezmes J, Correig X, et al. (2001) Electronic nose simulation tool centered on Spice. Sens Actuators B 76: 419-429.

23. Hammerichin O, Lund H, Hammerich O (2000) Organic Electrochemistry. (4thedn), Marcel Dekker, NY.

24. Lu Y, Li J, Han J, Ng HT, Binder C, et al. (2004) Room temperature methane detection using palladium loaded single-walled carbon nanotube sensors. Chem Phys Lett 391: 344-348.

25. Damgaard LR, Revsbech NP (1997) A microscale biosensor for methane containing methanotrophic bacteria and an internal oxygen reservoir. Anal Chem 69: 2262-2267.

26. Damgaard LR, Revsbech NP, Reichardt W (1998) Use of an oxygen-insensitive microscale biosensor for methane to measure methane concentration profiles in a rice paddy. Appl Environ Microb 64: 864-870.

27. Xiangfeng Ch, Donglia J, Yua G, Chenmoua Zh (2006) Ethanol gas sensor based on $CoFe_2O_4$ nano-crystallines prepared by hydrothermal method. Sens Actuators B 120: 177-181.

28. Lu F, Liu Y, Dong M, Wang X (2000) Nanosized tin oxide as the novel material with simultaneous detection towards CO, H2 and CH4. Sens Actuators B 66: 225-227.

29. Wang Sh H, Chou T Ch, Liu Ch Ch (2003) Nano Crystalline Tungsten Oxide NO_2 Sensor. Sens Actuators B 94: 343-351.

30. Chen Sh M, Wu MH, Thangamuthu R (2008) Preparation, Characterization, and Electrocatalytic Properties of Cobalt Oxide and Cobalt Hexacyanoferrate Hybrid Films. Electroanalysis 20: 178-184.

31. Zhang G, Liu M (2000) Effect of particle size and dopant on properties of SnO-based gas sensors. Sens Actuators B 69: 144-152.

32. Tan OK, Cao W, Hu Y, Zhu W (2004) Nano-structured oxide semiconductor materials for gas-sensing applications. Ceram Int 30: 1127-1133.

33. Tan OK, Cao W, Zhu W, Chai JW, Pan JS (2003) Ethanol sensors based on nano-sized a-Fe2O3 with SnO2, ZrO2,TiO2 solid solutions. Sens Actuators B 93: 396-401.

34. Choi SD, Min BK (2001) Co_3O_4-based isobutane sensor operating at low temperatures. Sens Actuators B 77: 330-334.

35. Korotcenkov GVM, Brinzari V, Tolstoy V, Schwank J, Cornet A, et al. (2004) Influence of Cu-, Fe-, Co-, and Mn-oxide nanoclusters on sensing behavior of SnO2 films. Thin Solid Films 467: 209- 214.

36. Jang JSR (1993) ANFIS: Adaptive-network-based fuzzy inference systems. IEEE Trans Syst Man Cybern 23: 665-685.

37. Ho YCh, Tsai ChT (2011) Comparing ANFIS and SEM in linear and nonlinear forecasting of new product development performance. Expert Syst Appl 38: 6498-6507.

38. Buragohain M, Mahanta Ch (2008) A novel approach for ANFIS modeling based on full factorial design. Appl Soft Comput 8: 609-625.

39. Takagi T, Sugeno M (1985) Derivation of fuzzy control rules from human operator's control actions, in: Proc IFAC Symp Fuzzy Inform. Knowledge Representation and Decision Analysis 55-60.

40. Meharrar A, Tioursi M, Hatti M, Boudghène Stambouli A (2011) A variable speed wind generator maximum power tracking based on adaptative neuro-fuzzy inference system. Expert Syst Appl 38: 7659-7664.

41. Sargolzaei J, Kianifar A (2010) Neuro-fuzzy modeling tools for estimation of torque in Savonius rotor wind turbine. Adv Eng Software 41: 619-626.

42. AliyariShoorehdeli M, Teshnehlab M, KhakiSedigh A (2009) Training ANFIS as an identifier with intelligent hybrid stable learning algorithm based on particle swarm optimization and extended Kalman filter. Fuzzy Sets Syst 160: 922-948.